An Attempt To Systematize the Vibrational Shifts in CO_2 Monomers and Dimers Trapped in Various Matrices

Andrei A. Vigasin,*,† Louise Schriver-Mazzuoli,‡ and André Schriver‡

Obukhov Institute of Atmospheric Physics, Russian Academy of Sciences, Pyzhevsky per. 3, Moscow 109017, Russia, and Laboratoire de Physique Moléculaire et Applications, Laboratoire propre du CNRS, UPR 136, Université Pierre et Marie Curie, Tour 13, case 76, 4 place Jussieu, 75252 Paris Cedex 05, France

Received: September 27, 1999; In Final Form: March 7, 2000

Infrared and Raman spectra of carbon dioxide monomers and dimers trapped in various matrices and in the gas phase are considered in an attempt to retrieve general regularities in vibrational shifts vs matrix properties. It is demonstrated that some useful conclusions can be drawn from an examination of the vibrational shifts as a function of the square root of the matrix material critical temperature. These correlations can be employed to roughly predict the positions of yet unknown vibrational origins or to obtain information on the nature of optically inactive hosts.

1. Introduction

As a simple polyatomic, the carbon dioxide molecule is one of the prototype systems for spectroscopic studies of molecular interactions. These studies are particularly important because carbon dioxide gas plays a crucial role in the absorption of radiation in the Earth's and other planetary atmospheres. Carbon dioxide is widely spread in the universe, and its ubiquitous role is evidenced by the detection of absorptions by free and adsorbed CO_2 molecules in the interstellar media. In this context, any minor changes in the spectrum of a carbon dioxide molecule due to environmental perturbations must be understood and thoroughly modeled.

Elementary intermolecular perturbations are due to pairwise interactions. Therefore, interest in the spectroscopic studies of a CO_2 molecule in weak van der Waals interaction with a variety of neutral atomic and molecular partners is very intense. In particular, the carbon dioxide dimers formed in molecular beams have been subjected to extensive high-resolution infrared[1−3] and Raman[4,5] observations. Also, the absorption spectra at high resolution are now available for bimolecular van der Waals complexes of CO_2 coupled to rare gas atoms[6,7] and to other polar and nonpolar molecular partners such as N_2,[8] C_2H_2,[9] OCS,[10] NH_3,[11] HCN,[12] H_2O,[13] CO,[14] H_2S,[15] N_2O,[16,17] HF, HCl, and HBr.[18,19] These observations have allowed a rigorous determination of the ground-state structure and vibrational frequency shifts in relevant van der Waals complexes.

Matrix isolation spectroscopy provides a wealth of information about the spectroscopic changes that occur with a specific molecule as a function of environmental host material, composition, and temperature. The vibrational origins of a CO_2 unit in the gaseous phase and in the solid are well-known (see Table 1). To establish these origins for carbon dioxide molecules trapped in various matrices, one must obtain vibrational spectra in which the observed features are thoroughly assigned. Vibrational spectra of matrix-isolated carbon dioxide are well documented.[20−27] Nevertheless, the data and band assignments differ somewhat in various publications, and no generally accepted model for vibrational shifts in CO_2 trapped in a variety of host matrices is available up to now.

TABLE 1: Reference Vibrational Origins (in cm^{-1}) of a CO_2 Monomer Measured in the Solid and Gas Phases

	ν_2	$\nu_1/2\nu_2$		ν_3	$\nu_3+\nu_1/\nu_3+2\nu_2$	
solid	659.3[a]	1273.3[a]	1384.6[a]	2344[b]	3600[b]	3712[b]
gas	667.4[a]	1285.4[a]	1388.2[a]	2349.14326[c]	3612.841[d]	3714.782[d]

[a] Ref 20. [b] Ref 30. [c] Ref 31. [d] Ref 7.

The present work pursues several goals. In the first part (see ref 27), new FTIR absorption spectra of CO_2 isolated in Ar and N_2 matrices are obtained at high resolution. This allows us to make our forthcoming considerations more reliable. In the second part, the data on vibrational shifts are systematized using the correlation established first by Luck et al.[28] for hydrogen-bonded species and then extended in ref 29. The correlation shows that the magnitude of the vibrational shifts varies linearly as a function of the square root of the critical temperature of the matrix material. The physical meaning of this correlation has been shown[28,29] to be attributable to the shift being determined by the host−guest interaction potential well depth, which, in turn, is known to correlate nicely with the square root of the host critical temperature. As shown in ref 29, the values characterizing free molecules in the gas phase may be included in the correlations at $T_c = 0$ K. This seems justified since, at $T_c \rightarrow 0$ K, the energy of the host−guest interaction is formally approaching zero. Therefore, the relevant values at $T_c = 0$ K must correspond to the unperturbed guest molecules. The present work shows that this correlation holds nicely for various vibrational modes of the carbon dioxide monomer and dimer. Moreover, a comparison is made between the matrix-induced shifts and those observed for the carbon dioxide dimer in molecular beams. It is shown that, generally, the gas-phase monomer and dimer data nicely meet the correlation retrieved from the spectroscopic observations in matrices. This makes it possible to predict the gas-phase dimeric vibrational shifts on the basis of known matrix shifts and vice versa. When the magnitude of a vibrational shift is known, it is then possible to

* To whom correspondence should be addressed. E-mail: vigasin@omega.ifaran.ru.
† Russian Academy of Sciences.
‡ Université Pierre et Marie Curie.

10.1021/jp993455n CCC: $19.00
Published on Web 05/20/2000

TABLE 2: Vibrational Shifts of a CO_2 Molecule in van der Waals Binary Complexes CO_2−M in the Gas Phase

weakly bound complex CO_2−M		$\sqrt{T_c}$	$\nu(CO_2)_{vdW} - \nu(CO_2)_{mon}$, cm^{-1}				
			$\nu_1/2\nu_2$		ν_3	$\nu_3+\nu_1/\nu_3+2\nu_2$	
	He	2.29	−	−	+0.095[a]	−	−
	Ne	6.67	−	−	+0.130[b]	+0.149[c]	+0.195[c]
	N_2	11.23	−	−	+0.485[d]	−	−
CO_2	Ar	12.29	−	−	−0.470[b]	−1.093[c]	−0.946[c]
	Kr	14.5	−	−	−0.884[b]	−1.973[c]	−1.758[c]
	Xe	17.02	−	−	−1.471[b]	−	−
	CO_2	17.44	−0.68[e]	−0.5[e]	+1.6289[f]	−1.294[g]	−0.850[g]

[a] Ref 8. [b] Refs 6 and 7. [c] Ref 7. [d] Ref 31. [e] Refs 4, 5, and 33. [f] Ref 3. [g] Ref 1. Also shown are the values of $\sqrt{T_c}$ in $K^{1/2}$ for relevant pure M substances (for D_2, $\sqrt{T_c} = 6.2$ $K^{1/2}$).

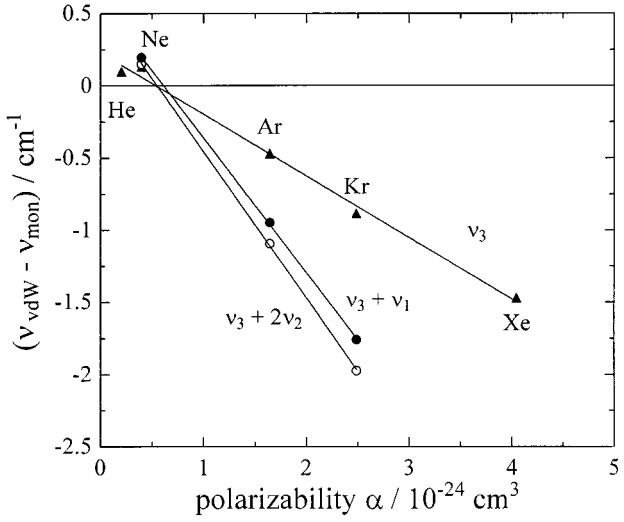

Figure 1. CO_2 intermolecular vibrational shifts in various Rg−CO_2 bimolecular complexes as a function of the polarizability of the rare gas atom. Triangles and empty and filled circles refer to various vibrational modes.

roughly identify the matrix material in which the CO_2 molecule is embedded.

2. Vibrational Shifts in Free Bimolecular Complexes Formed by the CO_2 Molecule

Prior to discussions of vibrational shifts in CO_2 molecules embedded in various matrices, it is instructive to summarize the data obtained for a variety of weakly bound CO_2 complexes in the gas phase. Table 2 shows a selection of vibrational shifts measured for a CO_2 molecule in pairwise interactions with rare gas atoms, with nitrogen, and with another CO_2 molecule (in a dimer). It is seen that the vibrations involving an antisymmetric stretch in the CO_2 molecule exhibit bathochromic (red) shifts in CO_2−Ar, CO_2−Kr, and CO_2−Xe complexes and hypsochromic (blue) shifts in CO_2−He, CO_2−Ne, CO_2−N_2, and CO_2−CO_2 complexes. The magnitude of the shift varies significantly, however, and the regularity is barely seen at first glance. Figure 1 shows that the ν_3 and $\nu_3+\nu_1/\nu_3+2\nu_2$ shifts caused by the interaction of the CO_2 molecule with rare gas (Rg) atoms are fairly linear as a function of atomic polarizability. This means that the shift in pair CO_2−Rg complexes is governed mainly by the long-range interaction potential terms. The magnitude of the shift changes from one vibrational mode to another, because the van der Waals interaction energy, which causes the vibrational origin to shift, is sensitive to vibrational excitation.

The shifts of the ν_3 antisymmetric stretch measured for CO_2−N_2 and $(CO_2)_2$ have a positive sign and can be qualitatively understood in terms of dominantly resonant interaction between

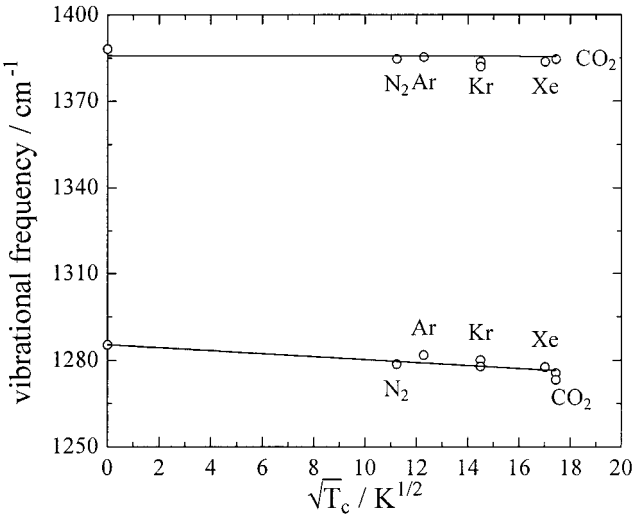

Figure 2. Measured positions of the CO_2 Fermi dyad as a function of $\sqrt{T_c}$ of the corresponding matrix material. Circles refer to monomer transitions in the gas phase, in matrices, and in the CO_2 crystal.

constituent monomer vibrations of the same or approximately the same frequency (see the relevant discussion by Weida et al.[32]). Note that, in contrast to ν_3, the vibrational shifts measured for the $\nu_1/2\nu_2$ and $\nu_3+\nu_1/\nu_3+2\nu_2$ Fermi-coupled modes of a CO_2 dimer are negative, although their magnitude can hardly be ascribed solely to the nonresonant effects.

3. Vibrational Shifts in Matrix-Trapped CO_2 and $(CO_2)_2$

3.1. Fermi-Coupled Transitions. A set of Raman data for vibrational origins of the Fermi-coupled $\nu_1/2\nu_2$ bands is available from Bier and Jodl[20] for CO_2 trapped in various matrices. Figure 2 shows that, when plotted as a function of the square root of the matrix material critical temperature T_c, the data nicely fit the straight-line dependencies. From a fitting procedure accounting for the gas-phase vibrational origins, the following approximate dependencies can be found (hereafter, ν is expressed in cm^{-1}, T in K):

$$\nu_1^{up} = 1388.2 - 0.26\sqrt{T_c} \qquad (1)$$
$$\nu_1^{low} = 1285.4 - 0.51\sqrt{T_c}$$

It is seen that the rate of decrease of the lower component frequency with the square root of the critical temperature is almost twice that for the upper component. Surprisingly, the position of the Fermi-coupled bands in crystalline carbon dioxide also fits these correlation dependencies. This means that the correlation remains valid extending from the gas phase to the solid, condensed phase via an intermediate range of various rare gas and nitrogen host matrices. We shall see below that this holds also for other vibrational modes for which more experimental data are available.

The correlation coefficient for the established linear dependencies (as well as for the majority of those in forthcoming sections) exceeds 0.8. However, in most cases, the number of available points (matrices) is less then 10, and therefore, statistics for these correlations are fairly insufficient. Despite the lack of statistically correct background, these correlations give an idea of the extent of a vibrational shift, which is useful to have for various reasons.

For the dimer vibrational shifts in the region of the $\nu_1/2\nu_2$ bands, only gas-phase data are available at the present time. CARS observations made by Huisken et al.[4,5] in a free jet

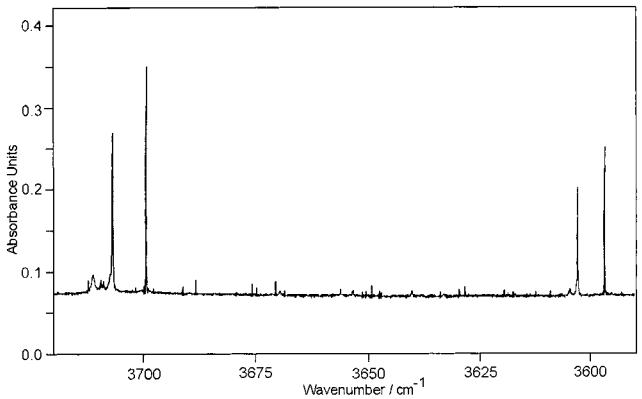

Figure 3. FTIR spectrum of CO_2 trapped in an Ar matrix (1/2000 at 11 K) in the region of the combination Fermi-coupled transitions.

expansion allowed the detection of the lower dimer component slightly red-shifted by -0.68 cm^{-1} relative to its monomeric progenitor. The red shift by -0.5 cm^{-1} of the upper Fermi-coupled band was established less reliably by Ramonat from the same group.[33] These observations were then strongly supported by FTIR examination of the $\nu_1/2\nu_2$ region in compressed carbon dioxide.[34] The positions of Q-branches in the infrared collision-induced spectra found by Baranov and Vigasin[34] are in excellent agreement with the above-mentioned findings by the CARS technique. From these results, one can infer that the $\nu_1/2\nu_2$ shifts upon dimer formation in a variety of matrices are merely on the order of 0.5 cm^{-1} and are always bathochromic.

In the combination Fermi-coupled $\nu_3+\nu_1/\nu_3+2\nu_2$ region, no CO_2 dimer data in matrices are available at the present time. It is known, however, that the vibrational shifts in a free dimer are -0.850 and -1.294 cm^{-1} for the ν_c^{up} and ν_c^{low} modes, respectively (subscript c hereafter means combination transition) (see Table 2). These numbers can be thought of as holding approximately for a matrix-trapped CO_2 dimer as well.

The typical FTIR absorption spectrum in this region for the CO_2 monomer trapped in an Ar matrix is shown in Figure 3. The lower and upper components of the Fermi doublet are each split into two bands, of which the lower-frequency component is narrower than the upper-frequency one. The gap between the components diminishes slightly when the temperature rises. These bands are due to the site splitting in the single- and double-site positions for the high- and low-lying components, respectively.[27] It is worth mentioning that no pronounced site splitting was reported for the Raman spectra of the main Fermi doublet $\nu_1/2\nu_2$.[20]

This site-splitting effect is clearly seen in the correlation plots depicted in Figure 4. A linear fit accounting for CO_2 gas-phase and solid-state values returns the following approximate relationships:

$$\nu_1^{up} = 3714.8 - 0.43\sqrt{T_c} \qquad (2)$$
$$\nu_1^{low} = 3612.8 - 0.71\sqrt{T_c}$$

The slopes of the upper and lower straight lines again differ approximately by a factor of 2. As can be seen from Figure 4, the double-site data for CO_2 in an Ar matrix drop slightly down off the linear correlation in comparison to the single-site data. We shall see below that the same is valid for the ν_3 antisymmetric stretch data.

3.2. ν_2 Bending Vibration. Table 3 summarizes our recent experimental results for the CO_2 monomer and dimer in argon

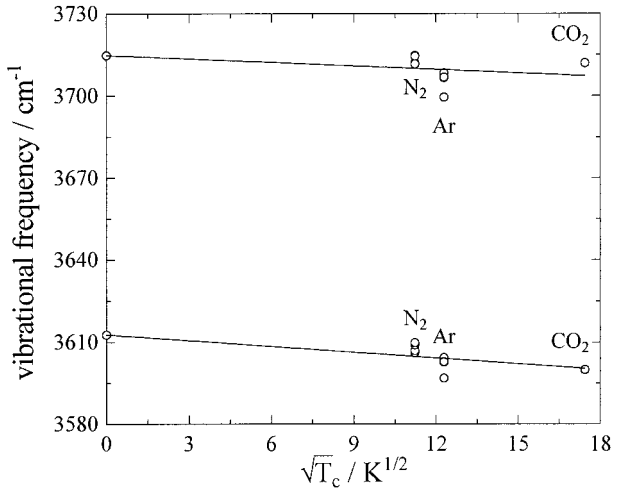

Figure 4. Measured positions of the CO_2 Fermi-coupled combination tones as a function of $\sqrt{T_c}$ of the corresponding matrix material. Circles refer to monomer transitions in the gas phase, in matrices, and in the CO_2 crystal. The solid line shows a least-squares fit of experimental points.

and nitrogen matrices,[27] as well as those previously reported in the literature referring to spectroscopic studies in various matrices.[20−25] The region of the ν_2 bending mode is sensitive to environmental perturbations. This makes the study of vibrational shifts in the ν_2 region particularly interesting for the applications (see, e.g., the works of Falk[35] and Strazzula et al.[36]). Figure 5 displays the vibrational frequencies of ν_2 for the monomer and the dimer trapped in different matrices plotted against $\sqrt{T_c}$. As discussed below in section 3.2.1, the dimer is characterized by two IR-active bending vibrations located lower and higher in the frequency scale relative to the monomer absorption band. For a monomer in an argon matrix, we report the position of the major single band at 661.9 cm^{-1} and the positions of the quadruple of components located at higher frequency that vanishes with increasing temperature.[27] In a nitrogen matrix, we do not observe dimer bands because of their weakness, a conclusion in agreement with that drawn in ref 22 (see relevant discussion in ref 27). As can be seen in Figure 5, despite minor deviations, the frequencies for both the monomer and the dimer nicely fit parallel straight-line dependencies. These deviations are attributed to slight misassignments in the original publications, site effects that can cause splitting comparable to the monomer−dimer splitting, and the effect of a temperature drift of relevant band centers. It is seen in Figure 5 that the monomer frequency in the gas phase is on the same linear plot that characterizes a CO_2 molecule embedded in various matrices and polycrystalline carbon dioxide. This finding justifies well the idea that the data for CO_2 in matrices can be extended to the gas phase. Independent fits over three separate sets of data points corresponding to the monomer and the dimer result in the following relationships:

$$\nu_2^{mon} = 667.4 - 0.46\sqrt{T_c}$$
$$\nu_2^{up} = 669.8 - 0.48\sqrt{T_c} \qquad (3)$$
$$\nu_2^{low} = 665.6 - 0.44\sqrt{T_c}$$

From these formulas, the yet unknown dimer vibrational origins in the gas phase can be predicted as $\nu_2^{up} = 669.8$ cm^{-1} and $\nu_2^{low} = 665.6$ cm^{-1}. Let us briefly comment on the nature of this splitting.

TABLE 3: Available Literature Data on the Vibrational Features Observed in the IR Spectra of CO_2 Trapped in Various Matrices[a,b]

	ν_2		$\nu_1/2\nu_2$		ν_3		$\nu_3+\nu_1/2\nu_2$	
matrix	cm^{-1}	assignment[c]	cm^{-1}	assignment[c]	cm^{-1}	assignment[c]	cm^{-1}	assignment[c]
D_2	663.0[d]	dim			2344.0[d]	mon		
	665.05[d]	mon						
	665.45[d]	mon						
	666.3[d]	dim						
	666.8[d]	dim						
N_2	657.4[h]	dim	1278.7[g]	mon	2348.1[h]	mon	3606.2[h]	mon
	660.6[e]	pair	1384.7[g]	mon	2348.6[e]	mon	3607.0[f]	mon
	662.2[h]	mon			2349.0[f]	mon	3609.1[f]	mon
	662.3[e,f]	mon			2349.2[f]	pair	3609.6[h]	mon
	664.3[e]	pair			2351.1[f]	dim	3711.6[f]	mon
							3712.0[h]	mon
							3714.5[f]	mon
							3714.7[h]	mon
Ar	659.6[i]	dim	1281.8[g]	mon	2331.2[h]	dim	3596.9[f]	mon
	659.9[e,f]	dim	1385.3[g]	mon	2338.8[e]	mon	3602.7[h]	mon
	660.3[h]	dim			2339[i,k]	mon	3602.9[f]	mon
	661.0[e]	dim			2339.1[f]	mon	3604.4[h]	mon
	661.3[h]	mon			2339.9[f]	dim	3699.5[f]	mon
	661.8[i]	mon			2340.2[f]	mon	3706.6[h]	mon
	661.9[e,f]	mon			2340.5[k]	mon	3708.3[h]	mon
	662.1[h]	mon			2342.0[f]	dim	3706.8[f]	mon
	663.3[h]	mon			2344.1[h]	mon		
	663.4[e,f,i]	mon			2344.5[e,i]	mon		
	663.5[f]	mon			2345.0[k]	mon		
	663.7[f]	mon			2345.05[f]	mon		
	663.8[f]	mon			2346.5[i]	dim		
	664.1[e]	dim			2346.7[k]	mon		
	664.2[i]	dim			2347.7[f]	dim		
	664.4[f]	dim						
	665.1[h]	dim						
Kr	658.6[i]	dim	1277.9[j]	mon	2336.5[i]	mon		
	660.2[i,j]	mon	1280.1[g]	mon	2340.5[i]	mon		
	661.2[i]	mon	1382.0[j]	mon	2342.2[j]	mon		
	662.2[i]	dim	1383.7[g]	mon	2342.5[i]	dim		
	662.6[j]	mon			2344.0[j]	mon		
Xe	658.5[i]	dim	1277.7[g]	mon	2336[i]	dim		
	661.2[i]	dim	1383.7[g]	mon	2334.5[i]	mon		
CO_2	659.3[g]		1273.3[g]		2344[l]		3600[l]	
			1384.6[g]				3712[l]	

[a] Note that experiments carried out by different authors refer to different temperature, as indicated by the accompanying footnote. [b] Data for crystalline CO_2 are shown in bottom row. [c] Original assignment of vibrational features to monomers, dimers, or pairs. [d] Irvine and Pullin,[21] $T = 6$ K. [e] Fredin et al.,[22] $T = 20$ K. [f] Schriver et al.,[27] $T = 11$ K. [g] Bier and Jodl,[20] $T = 15$ K. [h] Nxumalo and Ford,[24] $T = 17$ K. [i] Guasti et al.,[23] $T = 9$ K. [j] Loewenschuss and Givan,[25] $T = 20$ K. [k] Knözinger et al.,[26] $T = 12$ K. [l] Barnes and Gough.[30]

3.2.1. Harmonic Vibrations in a Dimer. The ground-state structure of a CO_2 dimer (see Figure 6) belongs to the C_{2h} symmetry point group and is often characterized as a slipped parallel configuration. In a monomer, the ν_2 bending mode is doubly degenerate. In a dimer, this mode splits into four vibrations having A_g, A_u, B_g, and B_u symmetries. Of these, one in-plane B_u and one out-of-plane A_u vibrations are active in infrared absorption. Figure 5 shows that an increase in the intermolecular interaction energy, which correlates with the square root of the critical temperature, causes a red shift in the monomer bending frequency. This means that the intermolecular interaction in a dimer must result in a decrease in the free monomer carbon dioxide bending force constant $K_{\gamma\gamma}$. When a dimer is formed, the in-plane $K_{\gamma_{\parallel}\gamma_{\parallel}}$ and out-of-plane $K_{\gamma_{\perp}\gamma_{\perp}}$ bending force constants vary at different rates, namely, $K_{\gamma_{\parallel}\gamma_{\parallel}}$ changes more significantly than does $K_{\gamma_{\perp}\gamma_{\perp}}$. To estimate this difference in force constants, we solved the inverse vibrational problem for a dimer using a set of intramolecular monomer and intermolecular dimer force constants currently available from the literature and listed in Table 4. Our goal was to vary $K_{\gamma_{\parallel}\gamma_{\parallel}}$ and $K_{\gamma_{\perp}\gamma_{\perp}}$ in an independent way in order to reproduce the shifts of $+2.4$ and -1.8 cm^{-1} predicted from the intercepts of the dimer linear plots in Figure 5 at $T_c = 0$ K. The in-plane $K_{\gamma_{\parallel}\gamma_{\parallel}}$ and out-of-plane $K_{\gamma_{\perp}\gamma_{\perp}}$ bending force constants for a dimer were found to decrease relative to the unperturbed $K_{\gamma\gamma}$ monomer value, as indicated in Table 4. Table 5 summarizes the results of our harmonic vibrational calculations. Interestingly, despite the fact that we kept the stretching force constants intact, the variation in the bending force constants caused a slight positive shift in the infrared-active antisymmetric stretching frequency, which is qualitatively in accord with the experimental observations.

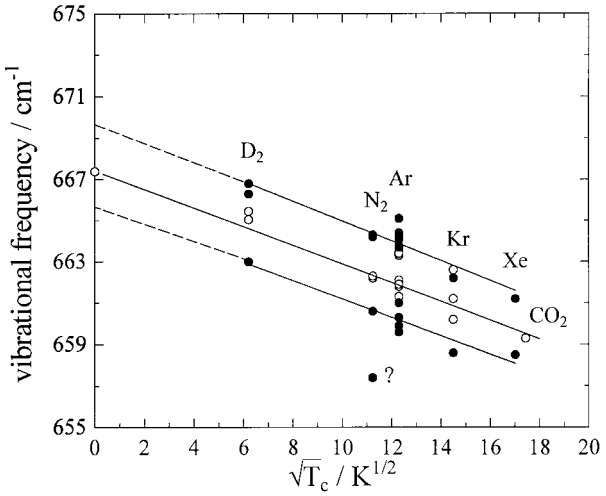

Figure 5. Measured positions of the spectroscopic features in the CO_2 bending region as a function of $\sqrt{T_c}$ of the corresponding matrix material. Empty and filled points refer to an assignment of observed peaks to CO_2 monomers and dimers, respectively, made by the authors of individual publications (see Table 3). Also shown are the monomer gas-phase and solid-phase data. The straight lines show the results of a least-squares fit. The question mark refers to a peak for which the assignment to a dimer in ref 24 seems unlikely in view of this correlation.

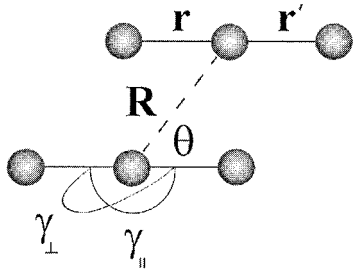

Figure 6. Ground-state structure of the carbon dioxide dimer and corresponding vibrational coordinates.

TABLE 4: Harmonic Force Constants for CO_2 Monomer and Centrosymmetric $(CO_2)_2$ Dimer

force constants, 10^8 N/m			
monomer		dimer	
rr	16.02[a]	rr	16.02[a]
rr'	1.26[a]	rr′	1.26[a]
$\gamma\gamma$	0.787[a]	$\gamma_{\perp}\gamma_{\perp}$	0.782[a]
		$\gamma_{\parallel}\gamma_{\parallel}$	0.760[a]
		RR	0.0387[b]
		Rθ	0.031[b]
		$\theta\theta$	0.129[b]

[a] This work. [b] Ref 1.

TABLE 5: Harmonic Vibrational Frequencies for CO_2 Monomer and Dimer and Comparison of Experimental and Calculated Vibrational Shifts in the Region of Bending Vibration

	symmetries and harmonic frequencies ν, cm^{-1}				frequency shifts ($\nu_{dim} - \nu_{mon}$), cm^{-1}	
	monomer		dimer			
	symmetry	ν_{harm}[a]	symmetry	ν_{harm}[b]	calculated	experimental
ν_1	Σ_g^+	1353.96	A_g	1353.96	0.0	−
			B_u	1353.96	0.0	−
ν_2	Π_u	673.25	A_g	666.69	−6.56	−
			B_u	675.76	+2.51	+2.4[c]
			A_u	671.29	−1.96	−1.8[c]
			B_g	671.29	−1.96	−
ν_3	Σ_u^+	2396.12	A_g	2396.12	0.0	−
			B_u	2396.25	+ 0.13	+1.69[d]

[a] Ref 37. [b] Calculated using force field shown in Table 4. [c] Values taken from Figure 5. [d] Ref 3.

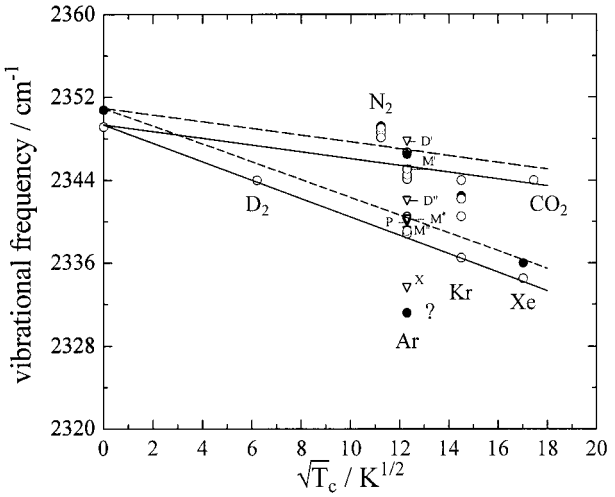

Figure 7. Measured positions of the CO_2 antisymmetric stretch vibration as a function of $\sqrt{T_c}$ of the corresponding matrix material. Empty and filled points refer to an assignment of observed peaks to CO_2 monomers and dimers, respectively, made by the authors of individual publications (see Table 3). Also shown are the monomer gas-phase and solid-phase data. The straight lines show the results of a least-squares fit. Empty triangles labeled by X, M″, P, M*, D″, M′, and D′ show peak positions in our experimental spectrum (see Figure 8 and ref 27). The question mark refers to a peak for which the assignment to a dimer in ref 24 seems unlikely in view of this correlation.

3.3. ν_3 Antisymmetric Stretch Vibration. The spectrum of matrix-isolated carbon dioxide in the region of the antisymmetric stretch, as in other regions, is complicated because of the existence of two distinct substitutional sites. Figure 7 demonstrates that, very roughly, two straight lines can be associated with the monomer shifts (one for the single site, the other one for the double site). They can be fit to the following relationships:

$$\nu_3^{up} = 2349.14 - 0.39\sqrt{T_c} \qquad (4)$$

$$\nu_3^{low} = 2349.14 - 0.725\sqrt{T_c}$$

Shifts are more pronounced for the double site, but the two lines converge to the same point at $T_c = 0$ K, corresponding to the frequency of a free monomer in the gas phase. The vibrational shift characterizing solid-phase CO_2 is located on the monomer straight line corresponding to the single-site position of a monomer. In the particular case of the ν_3 vibration, the shifts

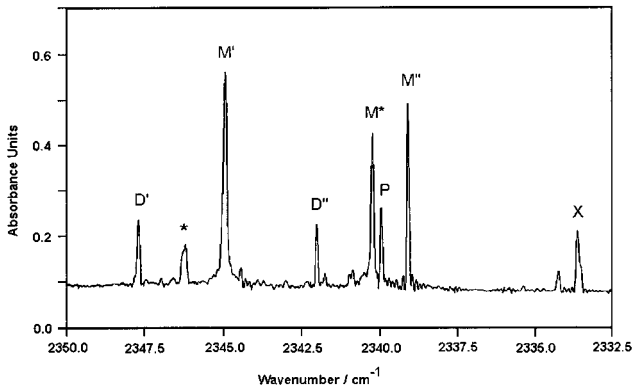

Figure 8. FTIR spectrum at 11 K in the ν_3 region of a CO_2/Ar mixture after annealing to 30 K for 45 min (CO_2/Ar = 1/10 000). Labels refer to the following assignment (see Figure 7 and ref 27): M, monomer; D′ and D″, dimers in two sites; P, pair; X, not assigned; and *, band due to N_2 impurity.

for a double-site position can be associated with a straight line connecting the free CO_2 and D_2 and the lower Ar, Kr, and Xe data points.

The position of the CO_2 antisymmetric stretch in a nitrogen matrix notably drops out of the linear correlations. One can speculate that such a strong relative positive shift might be due to a significant resonant effect, as it takes place in a free CO_2−N_2 van der Waals complex (see relevant discussion in section 2 above). As can be seen in Figure 4, qualitatively similar behavior is characteristic of the region of the monomer combination transitions $\nu_3+\nu_1/\nu_3+2\nu_2$.

The dimer band positions in matrices are difficult to identify because of the aggregation facility of CO_2 and the presence of impurity traces, as discussed in the first part of this work. Nevertheless, the dimer data can be tentatively represented as two blue-shifted lines parallel to the monomer single- and double-site lines, which converge at $T_c = 0$ K to the precisely established ν_3 band origin for the free gas-phase $(CO_2)_2$ dimer.[3]

In light of the correlations plotted in Figure 7, it is interesting to discuss our experimental results in the argon matrix.[27] As is shown in Figure 8, after annealing of a highly diluted CO_2/Ar sample, four main new bands appear at 2333.6 (X), 2339.9 (P), 2347.7 (D′), and 2342.0 cm^{-1} (D″), the two former being the first to be observed in controlled thermal diffusion. The P band was tentatively assigned to a CO_2 pair in adjacent sites, whereas the D′ and D″ bands were assigned to the dimer in two sites. Figure 7 shows that this attribution is in agreement with a variety of matrix data. However, other assumptions cannot be excluded. For example, the P band could be assigned to a dimer in one site, or the P and D′ bands could be ascribed to a dimer in two sites. Also, the assignment of the M* and D′ peaks to a dimer seems possible. Despite notable vagueness in assignment, the monomer and dimer peaks can be roughly positioned by assistance of Figure 7. For instance, the attribution of a peak labeled X in Figures 7 and 8 to a dimer can definitely be ruled out.

4. Conclusions

This work shows that the experimental data on CO_2 frequency shifts gained for different vibrational modes can be systematized using a correlation with the square root of the critical temperature, suggested for hydrogen-bonded species by Luck and associates.[28] Infrared and Raman data on transitions in the free CO_2 molecule, in carbon dioxide trapped in a variety of matrices, and in solid carbon dioxide satisfy these correlations. Minor

deviations and splittings might be explained in terms of different substitutional sites of trapped molecules. Moreover, currently available data for the free gas-phase CO_2 dimer generally fit these correlations, thus making it possible to roughly predict the relevant gas-phase dimer shifts. Also and inversely, the matrix-induced shifts can be predicted provided that the shifts in the gas phase are already known. It is shown, for instance, that the bending vibration in a dimer is split to red- and blue-shifted components located, respectively, $+2.4\ cm^{-1}$ upshift and $-1.8\ cm^{-1}$ downshift relative to the monomer band origin. The magnitude and even the sign of a shift vary significantly as a function of vibrational mode and local environment. This makes it possible to use the spectroscopically detected vibrational shifts in a chromophore molecule as an indicator of the host macroscopic properties.

A consideration of such correlations will be valuable for subsequent studies of vibrational shifts in a variety of chromophore−matrix pairs. Namely, the use of systematic dependencies will be of great importance for performing new vibrational measurements relevant to weakly bound van der Waals complexes either in the gas phase, in matrices, or deposited on nanoparticles.

As an evident application of the present analysis, one may note the identification of spectral signatures and host materials in the interests of remote sensing. Of course, the correlations are not sufficiently precise to determine exactly which matrix material is able to cause the observed shift for molecules adsorbed on the optically inactive host particles. Nevertheless, the use of the correlations established in the present paper allows an indication of certain intervals in which the host material critical temperature can be expected, in accord with the observed spectral shifts. Thus, new insight into the nature of the optically inactive host particles can be reached.

Acknowledgment. The authors appreciate the reviewers of this paper for attentive reading of the manuscript and valuable suggestions. Partial financial support from RFBR-CNRS project PICS 591 (98-05-22021) is gratefully acknowledged. A.A.V. thanks equally E. G. Tarakanova for assistance in doing vibrational calculations and LPMA, Université Pierre et Marie Curie, for its hospitality, and partial financial support through Grant RFBR 99-05-64215.

References and Notes

(1) Jucks, K. W.; Huang, Z. S.; Miller, R. E.; Fraser, G. T.; Pine, A. S.; Lafferty, W. J. *J. Chem. Phys.* **1998**, *88*, 2185.
(2) Jucks, K. W.; Huang, Z. S.; Dayton, D.; Miller, R. E.; Lafferty, W. J. *J. Chem. Phys.* **1997**, *86*, 4341.
(3) Walsh, M. A.; England, T. H.; Dyke, T. R.; Howard, B. J. *Chem. Phys. Lett.* **1987**, *142*, 265.
(4) Huisken, F.; Ramonat, L.; Santos, J.; Smirnov, V. V.; Stelmakh, O. M.; Vigasin, A. A. *J. Mol. Struct.* **1997**, *410*, 47.
(5) Vigasin, A. A.; Smirnov, V. V.; Ramonat, L.; Huisken, F. *Khim. Phys.* **1998**, *17*, 144 (in Russian).
(6) Randall, R. W.; Walsh, M. A.; Howard, B. J. *Faraday Discuss.* **1988**, *85*, 13.
(7) Pine, A. S.; Fraser, G. T. *J. Chem. Phys.* **1988**, *89*, 100.
(8) Walsh, M. A.; Dyke, T. R.; Howard, B. J. *J. Mol. Struct.* **1988**, *189*, 111.
(9) Huang, Z. S.; Miller, R. E. *Chem. Phys.* **1989**, *132*, 185.
(10) Novick, S. E.; Suenram, R. D.; Lovas, F. J. *J. Chem. Phys.* **1988**, *88*, 687.
(11) Fraser, G. T.; Leopold, K. R.; Klemperer, W. *J. Chem. Phys.* **1984**, *81*, 2577.
(12) Leopold, K. R.; Fraser, G. T.; Klemperer, W. *J. Chem. Phys.* **1984**, *80*, 1039.
(13) Peterson, K. I.; Klemperer, W. *J. Chem. Phys.* **1984**, *80*, 2439.
(14) Legon, A. C.; Suckley, A. P. *J. Chem. Phys.* **1989**, *91*, 4440.
(15) Rice, J. K.; Coudert, L. H.; Matsumura, K.; Suenram, R. D.; Lovas, F. J.; Stahl, W.; Pauley, D. J.; Kukolich, S. G. *J. Chem. Phys.* **1990**, *92*, 6408.
(16) Leung, H. O. *J. Chem. Phys.* **1998**, *108*, 3955.
(17) Dutton, C.; Sazonov, A.; Beaudet, R. A. *J. Phys. Chem.* **1996**, *100*, 17772.
(18) Lovejoy, C. M.; Schuder, M. D.; Nesbitt, D. J. *J. Chem. Phys.* **1987**, *86*, 5337.
(19) Sharpe, S. W.; Zeng, Y. P.; Wittig, C.; Beaudet, R. A. *J. Chem. Phys.* **1990**, *92*, 943.
(20) Bier, K. D.; Jodl, H. J. *J. Chem. Phys.* **1987**, *86*, 4406.
(21) Irvine, M. J.; Pullin, A. D. E. *Aust. J. Chem.* **1982**, *35*, 1961.
(22) Fredin, L.; Nelander, B.; Ribbegård, G. *J. Mol. Spectrosc.* **1974**, *53*, 410.
(23) Guasti, R.; Schettino, V.; Brigot, N. *Chem. Phys.* **1978**, *34*, 391.
(24) Nxumalo, L. M.; Ford, T. A. *J. Mol. Struct.* **1994**, *327*, 145.
(25) Loewenschuss, A.; Givan, A. *Spectrosc. Lett.* **1977**, *10*, 551.
(26) Knözinger, E.; Beichert, P. *J. Phys. Chem.* **1995**, *99*, 4906.
(27) Schriver, A.; Schriver-Mazzuoli, L.; Vigasin, A. A. *Vib. Spectrosc.* **2000**, *23*, 83.
(28) Behrens-Griesenbach, A.; Luck, W. A. P.; Schrems, O. *J. Chem. Soc., Faraday Trans.* **1984**, *280*, 579.
(29) Huisken, F.; Kaloudis, M.; Vigasin, A. A. *Chem. Phys. Lett.* **1997**, *269*, 235.
(30) Barnes, J. A.; Gough, T. E. *J. Chem. Phys.* **1987**, *86*, 6012.
(31) Weida, M. J.; Sperhac, J. M.; Nesbitt, D.; Hutson, J. M. *J. Chem. Phys.* **1994**, *101*, 8351.
(32) Weida, M. J.; Sperhac, J. M.; Nesbitt, D. *J. Chem. Phys.* **1995**, *103*, 7685.
(33) Ramonat, L. Ph.D. Thesis, University of Göttingen, Göttingen, Germany, 1997; MPI für Strömungsforschung, Report No. 3/1997.
(34) Baranov, Y. I.; Vigasin, A. A. *J. Mol. Spectrosc.* **1999**, *193*, 319.
(35) Falk, M. *J. Chem. Phys.* **1987**, *86*, 560.
(36) Strazzulla, G.; Nisini, B.; Leto, G.; Palumbo, M. E.; Saraceno, P. *Astron. Astrophys.* **1998**, *334*, 1056.
(37) Sverdlov, L. M.; Kovner, M. A.; Krainov, E. P. *Vibrational Spectra of Polyatomic Molecules*; Nauka: Moscow, 1979 (in Russian).